ResearchGate

See discussions, stats, and author profiles for this publication at: https://www.researchgate.net/publication/7239281

# Single molecule fluorescence imaging of the photoinduced conversion and bleaching behavior of the fluorescent protein Kaede

**ARTICLE** *in* MICROSCOPY RESEARCH AND TECHNIQUE · MARCH 2006

Impact Factor: 1.15 · DOI: 10.1002/jemt.20283 · Source: PubMed

CITATIONS
13

READS
20

**4 AUTHORS**, INCLUDING:

Petra S Dittrich
ETH Zurich
**117** PUBLICATIONS **3,173** CITATIONS
SEE PROFILE

Eugene P. Petrov
Max Planck Institute of Biochemistry
**67** PUBLICATIONS **1,555** CITATIONS
SEE PROFILE

Petra Schwille
Max Planck Institute of Biochemistry
**334** PUBLICATIONS **15,802** CITATIONS
SEE PROFILE

Available from: Eugene P. Petrov
Retrieved on: 26 January 2016

# Single Molecule Fluorescence Imaging of the Photoinduced Conversion and Bleaching Behavior of the Fluorescent Protein Kaede

S.P. SCHÄFER,[1] P.S. DITTRICH,[2] E.P. PETROV,[1] AND P. SCHWILLE[1]*
[1]*Institute of Biophysics / BIOTEC, TU Dresden, Tatzberg 47-51, D-01307 Dresden, Germany*
[2]*Department of Miniaturization, Institute for Analytical Sciences (ISAS), D-44139 Dortmund, Germany*

*KEY WORDS* single-molecule fluorescence microscopy; fluorescent proteins; Kaede; photoactivation; photophysics

*ABSTRACT* Photoconversion and photobleaching behavior of the fluorescent protein Kaede immobilized in polyacrylamide gel matrix at room temperature was studied by single molecule widefield fluorescence microscopy. Photobleaching kinetics of Kaede molecules upon excitation at 488 nm showed slight heterogeneity, suggesting the presence of different protein conformations and/or the distribution of local environments in the gel matrix. Statistical analysis of intensity trajectories of single molecules revealed four major types of fluorescence dynamics behavior upon short illumination by a violet light pulse (405 nm). In particular, two types of photoswitching behavior were observed: the green-to-red photoconversion (4% of Kaede molecules) and the photoactivation of green fluorescence without emission of red fluorescence (13%). Two other major groups show neither photoconversion nor red emission and demonstrate photoinduced partial deactivation (43%) and partial revival (30%) of green fluorescence. The significantly lower green-to-red conversion ratio as compared with bulk measurements in aqueous solution might be induced by the immobilization of the protein molecules within a polyacrylamide gel. Contrary to Ando et al. (Proc Natl Acad Sci 2002;99:12651–12656), we found a significant increase in green fluorescence emission upon illumination with 405-nm light, which is typical for GFP and related proteins. *Microsc. Res. Tech. 69: 210–219, 2006.* © 2006 Wiley-Liss, Inc.

## INTRODUCTION

Since the first successful cloning of genetically-encoded fluorescent proteins based on the Green Fluorescent Protein (GFP) of the jellyfish *Aequorea victoria*, a plethora of fluorescent proteins (FPs) were developed as mutants of GFP or similar coelenterate proteins during the last decade (Zhang et al., 2002). Because of their minimum interference with intracellular processes they are widely used for labeling proteins in vivo by forming protein fusion constructs. Applications like monitoring signaling pathways or intracellular trafficking have made the fluorescent proteins an invaluable tool for fluorescence-based investigations in molecular biology.

Because of undesirable autofluorescent background that is usually found in biological cells in the green–yellow spectral range, development of fluorescent markers with a red-shifted emission wavelength is of high importance. In addition to the red fluorescent protein cloned from the *Discosoma* coral (DsRed or drFP583) (Matz et al., 1999), other proteins emitting in the red spectral range have been found, including, e.g., mRFP1 (Campbell et al., 2002) and eqFP611 (Wiedenmann et al., 2002). Contrary to the tetrameric DsRed (Shaner et al., 2004), the latter are monomers, and therefore, are much better suitable for the use as markers in fusion constructs.

Recently, another group of fluorescent proteins with altered spectroscopic properties has acquired considerable attention. Contrary to the previously mentioned proteins exhibiting a sprectral red-shift upon maturation, proteins like Kaede (Ando et al., 2002), mcavRFP (Shagin et al., 2004), rfloRFP (Shagin et al., 2004), DendFP (Pakhomov et al., 2004), EosFP (Nienhaus et al., 2005; Wiedenmann et al., 2004), and Dronpa (Habuchi et al., 2005) show a light-triggered red shift, which can be reversible, as in case of Dronpa. Compared to carbocyanine dyes, where photoswitching can only take place in the presence of triplet quenchers and absence of oxygen, recombinant proteins can also be used in the intracellular environment. Furthermore, photoswitchable proteins may provide striking experimental benefits in a cellular context where fluorescence-based single molecule tracking is difficult: by switching the fluorescence activity on at one specific time point, movement of single molecules in a tightly confined region of cellular compartments can be traced much easier (Ando et al., 2002).

*Correspondence to: P. Schwille; Institute of Biophysics/BIOTEC, TU Dresden, Tatzberg 47-51, D-01307 Dresden, Germany.
E-mail: schwille@biotec.tu-dresden.de

Received 10 September 2005; accepted in revised form 5 October 2005

Contract grant sponsors: BMBF, DFG.; Contract grant sponsor: EFRE; Contract grant number: 4-0123.55-20-0370-03/3.

DOI 10.1002/jemt.20283

Published online in Wiley InterScience (www.interscience.wiley.com).

© 2006 WILEY-LISS, INC.

All fluorescent proteins known today contain one or more 11-stranded β-barrels with a central helix in which the fluorophore, 4-(*p*-hydroxybenzylidene)-5-imidazolinone is shielded from the environment (Ormö et al., 1996). Whereas in GFP, the fluorophore is autocatalytically formed by a single oxidative cyclization of the triplet Ser-Tyr-Gly, the formation of the fluorophore in DsRed and eqFP611 requires further maturation in another oxidation step (Gross et al., 2000; Wiedenmann et al., 2002). The fluorophore formation in the photoswitchable proteins proceeds in two steps, however, the red-emitting fluorophore is formed upon absorption of violet light of around 400 nm (Ando et al., 2002). According to a mechanism suggested by Mizuno et al. (2003), the green fluorophore is cleaved between the amide nitrogen and the α-carbon in His62 upon excitation, via a β-elimination reaction which requires the catalytic activity of the whole intact protein. A subsequently formed double bond results in an extension of the π-conjugated electron system thus producing a new red emitting fluorophore.

As is well known, fluorescence can deliver valuable information on structural dynamics and photophysical behavior of fluorophores. A striking feature of many FPs found so far is the dual band absorption at about 390–400 nm causing weak fluorescence around 460 nm and at 475–510 nm, which gives the strong fluorescence peak at 508 nm (Chattoraj et al., 1996). Investigations based on fluorescence spectroscopy have shown that this can be attributed to two distinct chemical forms, a protonated (neutral) and a deprotonated (anionic) form, with a pH dependent relative intensity of the respective absorption and emission peaks (Lossau et al., 1996). Understanding the intricate photophysics of GFP and its mutants—in particular, the influence of the structure and the conformational dynamics on the fluorescence characteristics of the proteins–offers the possibility to design FPs with desired properties. However, in an ensemble, fluorescent proteins often display heterogeneity related to the chemical structure and the electronic state of the molecules. Therefore, fluorescence studies on the single molecule level (Weiss, 1999; Xie et al., 1998) can provide more detailed information than conventional fluorescence techniques based on measuring parameters of ensembles of molecules. In particular, the reversible conversion reactions in FPs between the protonated and the deprotonated states taking place on short time scales (so-called flickering) were proven for the first time by single molecule fluorescence methods, including single molecule microscopy (Schmidt et al., 1995; Dickson et al., 1997; Kues et al., 2001) and fluorescence correlation spectroscopy (Haupts et al., 1998; Malvezzi-Campeggi et al., 2001; Schwille et al., 1999).

In our previous work (Dittrich et al., 2005), we utilized fluorescence correlation spectroscopy to investigate the fast flickering dynamics of Kaede protein which proved to be pH-dependent for the green (grKaede) but not for the red (rKaede) form. Based on a microchannel continuous flow technique, the conversion reaction was studied and a conversion time of ~40 ms was determined. Studies of very slow processes, however, were not accessible by these techniques.

In the present work, we approached the photoinduced green–red conversion process, fluorescence photobleaching, and long-time blinking behavior of the Kaede protein by spectrally resolved fluorescence imaging of single Kaede molecules immobilized in a polyacrylamide gel matrix.

## MATERIALS AND METHODS

### Protein Treatment and Sample Preparation

Green Kaede protein, kindly provided by Prof. A. Miyawaki, was produced and purified as described before (Ando et al., 2002). It was stored at −80°C in buffer (10 mM Tris-HCl, 1 mM EDTA, 150 mM NaCl, pH 8.0). Before the experiments, the protein was diluted in 10 mM MOPS-buffer, pH 7.0. For imaging measurements, green Kaede protein was immobilized in polyacrylamide (PAA) gel at nanomolar concentrations following the protocol of Dickson et al. (1996). The protein concentration in the PAA gel was 71 nM for bulk measurements and between 0.9 and 7.6 nM for single molecule measurements.

Samples were prepared by mixing 1.0 μL Kaede protein solution in 10 mM MOPS buffer (pH 7.0) with 99 μL gel mix (in 1 mL gel mix: 550 μL acryl amide:bis-acryl amide, 38:2, 40%; 2.5 μL *N,N,N′,N′*-tetramethylethylendiamine, 447 μL MOPS-Tris-buffer). Coverslips were cleaned carefully by ultrasonication in a detergent solution, a rinsing cascade (purified water (LiChrosolv, Merck, Darmstadt, Germany), propanol, acetone, and purified water), and a final exposure to an oxygen plasma. Sample solution in the amount of 1.0 μL was sandwiched in between two coverslips after adding 0.5 μL of ammonium persulfate solution (4%) to start the polymerization reaction. After a few minutes waiting time, the gel was polymerized.

Bulk fluorescence emission spectra of the green and the red protein were acquired using protein solution in a micromolar concentration diluted in 10 mM MOPS-buffer, pH 7.0.

All measurements were carried out at room temperature (22°C).

### Optical Setup

The experimental setup (Fig. 1) for the single molecule imaging experiments is based on a wide field epifluorescence configuration using an inverted Olympus IX-50 microscope, equipped with either an oil or water immersion objective with a high numerical aperture (60X/1.40 UPlanApo oil immersion; 60X/1.20 UPlanApo water immersion, Olympus), similar as has been used by Kues et al. (2001). The setup was equipped with an ultra-sensitive high speed CCD camera (CoolSnap HQ, Roper Scientific, 1392 × 1040 pixels chip, pixel size: 6.45 × 6.45 $\mu m^2$) and an acousto-optic tunable filter (AA.MOD.4C, A.A Sa, St-Rémy-Lès-Chevreuse, France). For probing the fluorescence emission, a 488 nm line of an Ar/Kr ion laser (Innova 70, Coherent) was used, whereas for initiating the photochemical conversion, a blue laser diode (Laser 2000, Wessling, Germany) emitting at 405 nm was utilized. Both laser beams were superimposed by a dichroic mirror (405 DCLP, all filters and dichroics purchased from AHF, Tübingen, Germany), passed a λ/4-plate, were expanded and focused on the back focal plane of the objective, thus providing a homogeneous illumination of the region of interest (ROI). In front of the objective a custom-made dichroic mirror (495dcx) was installed

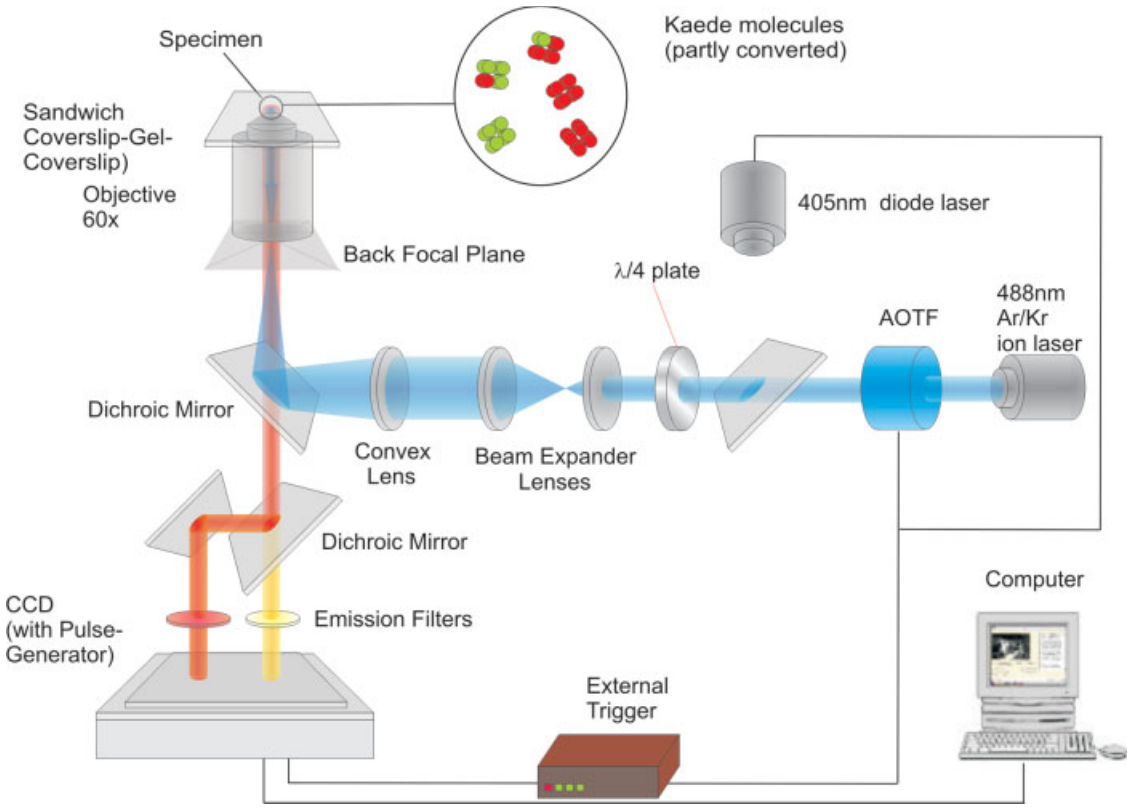


Fig. 1. Sketch of the wide field epifluorescence setup for single molecule imaging microscopy (see text for details). [Color figure can be viewed in the online issue, which is available at www.interscience.wiley.com.]

to separate the fluorescence emission from the excitation light. In the emission beam path, a dichroic beam splitter (D565) together with a band pass (D535/50F) and a long-pass filter (OG570) were used to separate the green and the red emission channels. Green and red fluorescence was imaged at the same time on different regions of the CCD chip. The lasers and the CCD camera were externally triggered in a coordinated way. For aligning the green and red images on the CCD chip, beads emitting in both spectral channels were immobilized on coverslips in order to determine the lateral shift vector between corresponding pixels. Image acquisition was performed using commercial software (WinSpec/32, Roper Scientific, USA).

Series of fluorescence images were acquired while illuminating the sample with 488 nm light pulses. In the following, each single image is referred to as frame. No illumination took place when the CCD camera was off, and vice versa. In one type of experiments, in between two selected frames one additional violet light pulse ($\lambda = 405$ nm) was applied to trigger the conversion process. In another type of experiments only 488 nm excitation pulses were used.

For acquisition of fluorescence spectra a glass fiber-coupled spectrometer (S2000, Ocean Optics) was used.

## Image Processing

To analyze and process image sequences obtained in experiments, we developed an interactive software tool programmed using the MATLAB-environment (The MathWorks, MA, USA), which was combined with a multidimensional image viewer (View5D, kindly provided by R. Heintzmann, http://wwwuser.gwdg.de/~rheintz/View5D/). Specific details of the image processing and analysis procedure will be published elsewhere. Briefly, after determining the lateral shift vector between the "red" and the "green" channels, the image sequences were inspected visually to select the ROI boundaries (size about 150 × 200 pixels). After correction for the fluorescent background in the first step, approximate positions of spots due to the emission of single molecules were determined automatically according to a predefined minimum intensity threshold. In the second step, an image of each spot was fitted with a 2D-Gaussian yielding the $x$- and $y$-spot positions and the spot integral intensity. It has to be emphasized that the spots were successfully immobilized in the gel matrix. The positions of the molecules obtained from the intensity fit did not vary more than $\pm 1$ pixel length over the course of the image series.

In the analysis, the spot width was set constant as determined by the PSF measured on subresolution size fluorescent beads. Spots having the same positions over the whole set of the images in both spectral channels were linked through the image stack resulting in a set of intensity trajectories in both spectral channels. The procedure outlined provides a reliable recognition and description of the spots, as is evident from the reconstructed image (Fig. 2) and the residuals between the original and the reconstructed images. All significant spots could be found and fitted automatically by

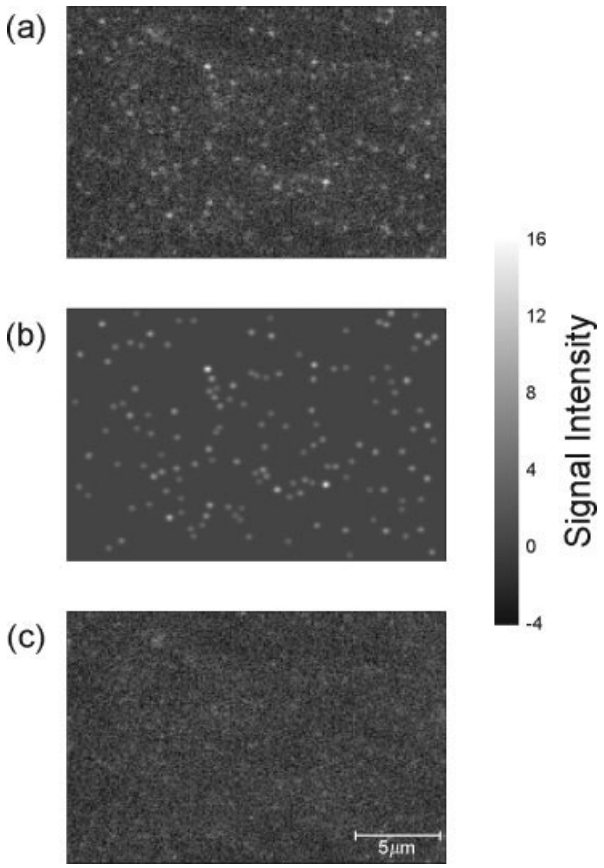


Fig. 2. Fluorescence microscopy image (150 × 200 pixels, 1 pixel = 108 × 108 $nm^2$) of Kaede molecules immobilized in PAA gel detected in the green spectral channel upon excitation at 488 nm light (3 ± 0.3 kW/$cm^2$, exposure time: 10 ms). Raw image (constant background subtracted) (**a**), image reconstructed by automatic spot detection and Gaussian fitting (**b**), and residuals (**c**).

supplying the algorithm with a user-defined labeling threshold.

## RESULTS AND DISCUSSION

### Flourescence of Kaede Protein in Polymer Gel Matrix

Our experimental procedure provided immobilization of Kaede protein molecules in a PAA gel (Dickson et al., 1996). Although the gel environment prevented diffusion of protein molecules, filling the gel pores with a buffer solution enabled mobility of the amino acid chain similar to that in aqueous solution. As a result, the Kaede protein molecules immobilized in the matrix showed fluorescence of two types (*vide infra*) as has been observed previously (Ando et al., 2002; Dittrich et al., 2005). Since we expected the photophysical properties of the protein molecules to be the same in the gel matrix as in the buffer solution, fluorescence emission spectra of the green and red form were measured in samples within aqueous buffer (Fig. 3) at micromolar protein concentrations. First, the grKaede protein spectrum was acquired. Then the solution was illuminated for several seconds with 405 nm light to photoconvert grKaede to rKaede. After that, a second fluorescence emission spectrum of the rKaede protein was taken.

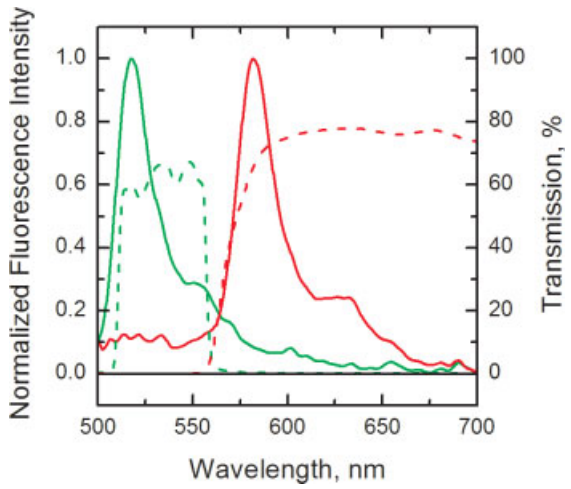


Fig. 3. Fluorescence emission spectra (solid curves) of green and red forms of Kaede protein and transmission spectra (dashed curves) of optical filters in the green and red detection channels. [Color figure can be viewed in the online issue, which is available at www.interscience.wiley.com.]

### Photobleaching Induced by 488 nm Light

Acquiring information about the fluorescent properties of a molecule generally involves (optical) excitation with subsequent detection of the emitted radiation. Besides the direct radiative decay into the (singlet) ground state (typically within less than 100 ns), there are also nonradiative ways of leaving the excited state, including a possible conversion to a long lived "dark" state from which nonradiative decay to the ground state can occur.

After a finite number of absorption-emission cycles, the fluorophore finally degrades ("bleaches") by an irreversible chemical reaction and loses its ability to fluoresce. In the case of grKaede, the intensity of the green fluorescence decreases slowly due to bleaching (by illumination with 488 nm light) as well as photoconversion (induced by violet light). Since the illumination intensity at 488 nm could not be decreased below a certain value due to limitations in the signal-to-noise ratio in the detected fluorescence signal, an accurate analysis of the photoconversion process requires a careful characterization of the bleaching behavior.

To characterize the photobleaching behavior, the fluorescence emission of grKaede molecules was recorded as a function of illumination time under conditions where no photoconversion was expected (diode laser blocked). Thirty frames of 200 × 200 pixel images were acquired during illumination of the samples by 10 ms pulses at 488 nm. Excitation intensity was set to 3 ± 0.3 kW/$cm^2$. After acquiring an image during a single 10 ms excitation pulse, each frame was transferred (read out) from the CCD to the computer within 50 ms. During this time (read-out time), no exposure of the sample to light took place. Each image obtained was analyzed as described earlier.

The number of grKaede spots found in the corresponding frames and the sum of the spot intensities are displayed as a function of illumination time with

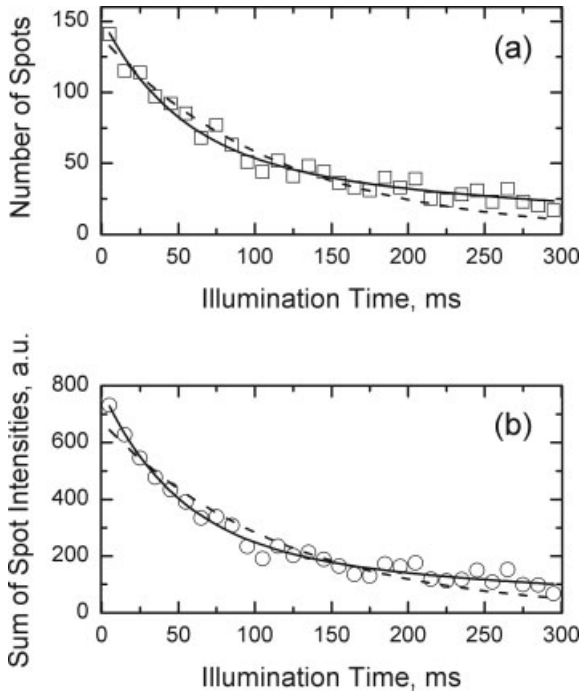


Fig. 4. Photobleaching kinetics of PAA gel-immobilized Kaede protein molecules: (**a**) number of spots detected in the image (open squares) and (**b**) sum of spot intensities (open circles) as a function of the illumination time. Also shown are single-exponential (dashed curves) and biexponential fits (solid curves). Excitation wavelength, 488 nm. Excitation power, 3 ± 0.3 kW/cm$^2$.

488 nm light in Figures 4a and 4b, respectively. As can be seen, both the detected number of spots and the sum of their intensities per frame decreases with increasing duration of illumination. These decays within the error limits follow the same dependence. Indeed, a least-squares-fit with a single-exponential decay model yielded the decay times of ≈132 and ≈116 ms for the number of molecules and their intensity, respectively. However, a much better fit can be obtained with a biexponential model: $X(t) = X(0)\,(\alpha \exp(-t/\tau_1) + (1-\alpha)\exp(-t/\tau_2))$ where $X(t)$ is either the number of spots in the ROI or their integral intensity. The biexponential model gives $\alpha \approx 0.32$, $\tau_1 \approx 0.06$ s, and $\tau_2 \approx 0.38$ s for the number of spots and $\alpha \approx 0.31$ $\tau_1 \approx 0.05$ s, and $\tau_2 \approx 0.35$ s for the sum of spot intensities.

Two conclusions can be drawn from these observations: First, while in general, the decay of the number of spots as well as the sum of intensities over illumination time is not surprising, the similarity of the decay rates shows that the photobleaching probability is virtually independent of the spot intensity.

Second, the non-monoexponential decay of the number of spots and their integral intensity might suggest the existence of at least two grKaede subspecies affected by photobleaching in a different way. (Since the fluorescent background was carefully removed during the image processing, its contribution can be excluded as reason for the non-single–exponential intensity decay.)

Apart from heterogeneities in the microenvironment of the molecules within the PAA gel (as observed for PVA gels by Habuchi et al., 2005), photophysical reasons specific for the Kaede protein and other GFP-mutants (Ando et al., 2002; Dickson et al., 1997; Jung et al., 2000; Patterson and Lippincott-Schwartz et al., 2002) could explain the presence of at least two fractions of protein molecules corresponding to two decay times of about 50 and 350 ms. The fast decaying fraction could be attributed to a type of molecules that are converted by the 488 nm excitation light into a dark state similar to Dronpa (Habuchi et al., 2005). The slower decaying species eventually bleach irreversibly into a non fluorescent dark state without previous conversion.

Negative controls with samples prepared as described earlier in which the protein solution was substituted by buffer solution showed a low fluorescent background constant over time. In particular, background fluorescence was the same before and after 405 nm illumination.

### Reaction Pathways Induced by 405 nm Light

After analyzing the photobleaching of the grKaede molecules by the 488 nm irradiation, we carried out a series of photoconversion experiments. By imaging the corresponding fluorescence signal of single protein molecules in the red and green channels as a function of time, we determine the temporal conversion behavior of grKaede to rKaede.

Since potential bleaching of the molecules because of excitation with the blue light could be detrimental to the analysis of photoconversion, the sample was illuminated in the following sequence: First, in step one, four two-color-images were taken with excitation by the blue (488 nm) light (excitation intensity: 0.6 ± 0.06 kW/cm$^2$ for 50 ms; read-out time for each image (illumination blocked): 100 ms). In the second step, the sample was exposed for 100 ms to a single flash of violet light ($\lambda$ = 405 nm; 0.15 ± 0.05 kW/cm$^2$). Directly following the 405 nm pulse, four more images with the excitation at 488 nm were collected as in step one. Except when exposed to violet light, the protein emission was recorded for every frame in both channels.

Unfiltered fluorescence images for a typical experiment of this type (background level subtracted) are displayed in Figure 5. Frames 1, 4, and 5 are shown in Figures 5a–5c, respectively. Inspection of the images shows that first, much fewer spots are visible in the red than in the green channel for all frames. This behavior is indeed expected for Figures 5a and 5b due to the absence of violet light during and before image acquisition for the frames 1–4. (The spots present in the red channel in Figures 5a and 5b had obviously converted before the triggering light pulse was applied.) Second, in both channels a moderate decrease in the number of spots is visible between the upper two pairs of images, reflecting photobleaching from frames 1–4. However, after illumination with 405 nm light between frame 4 and 5, a strong increase in the spot number can be seen in both channels. In addition to the expected green-to-red conversion leading to an increase in the number of "red" (and lowering the number of "green") emitting molecules, a large number of previously nonfluorescing molecules appears in the green channel (Fig. 5c). Since the absorbance of rKaede at 488 nm is roughly half as high as for grKaede, the ratio of the emission intensities

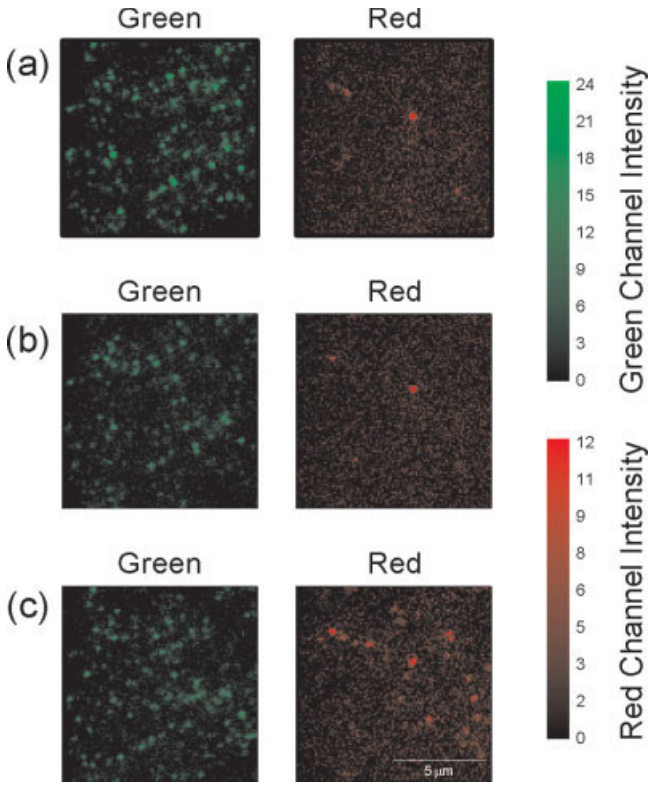


Fig. 5. Observation of the photoconversion and photobleaching of single Kaede protein molecules immobilized in PAA gel. Unfiltered background-corrected images (**a**), (**b**), and (**c**) correspond to frames 1, 4, and 5. Images are acquired with excitation at 488 nm (0.6 ± 0.06 kW/cm$^2$, exposure time: 50 ms). The violet light pulse (405 nm, 0.3 ± 0.03 kW/cm$^2$, duration 100 ms) was applied between frames 4 (**b**), and 5 (**c**). [Color figure can be viewed in the online issue, which is available at www.interscience.wiley.com.]

should be expected to be similar. Thus, in Figures 5 and 6, the color bars in the red and green channels scale 1:2.

This activation of nonfluorescent molecules to green emission by radiation around 400 nm had been previously observed in the case of GFP and its mutants (Habuchi et al., 2005; Jung et al., 2001). Surprising to us was the high amount of activated green compared to green-to-red photoconverted Kaede, which we quantified in a further step below.

It should be mentioned that the green-to-red conversion process, as well as the nonfluorescent-to-green activation is completed within frame 5. An image analysis has shown that no new spots appear in the frames 6–8 that were not present already in frame 5 (data not shown). The images shown in Figure 5 represent a quarter of the area that was subjected to a statistical analysis of spot behavior, as discussed in what follows.

To quantify the conversion and activation processes, the full frames 1–8 (200 × 190 pixels) were analyzed as described earlier. For each spot detected in any frame, the $x$- and $y$-positions and the intensity were determined in all eight frames in both channels. The resulting intensity trajectories were sorted into 16 different groups, depending on whether spots were active in the first or last four frames in the red or green channels (see Appendix). For each trace in both channels, the mean intensities in frames 1–8 were compared to an empirical threshold value to determine whether the particular spot is on average "active" or "inactive" in the specific channels. The threshold value was chosen to be the same for both channels because it was largely determined by the variance of the read-out noise of the CCD camera, which is independent of the spectral range.

A spot had to show activity at least in one of the spectral channels to be included in the analysis at all. If the spot is "active," the ratio between the mean intensities for the frames 1–4 and 5–8 was compared against the second threshold estimated based on the bleaching experiments described earlier determining if photoinduced switching occurs.

Depending on the ratio of the mean intensities in frames 1–4 and 5–8, we can classify the intensity trajectories in each of the channels into the classes "on/on," "on/off," "off/on," and "off/off". With this notation, for example, the expression "green on/off" refers to a spot in the green channel being on average "on" during the frames 1–4, and on average "off" during the frames 5–8.

Combination of the classes for the green and the red channels yields 16 groups in which the trajectories were sorted. Although 16 possible combinations of green/red emission characteristics existed, 90% of all the traces belonged to only one of four categories.

Upon sorting, the spots were reconstructed as noise-free images and concatenated. Altogether 534 different single molecule traces were detected and analyzed. To show the typical dynamics of spots, 15 representative traces are displayed in Figures 6a–6d for each group. As in Figure 5, in each plot the spots' intensities are presented in two blocks, for the green and red channels.

Figure 6a shows 15 trajectories grouped by the property "green on/off," "red off/on". In total, 22 of 534 trajectories (4%) were classified for this group. All traces display a strong increase in red fluorescence after being illuminated with violet light (after frame 4); Simultaneously, in all traces the green signal is substantially reduced from frame 5 on. At the same time, notice that several of the molecules show some red emission even before the activation by the violet pulse (e.g., spot 9). On the other hand, one can observe some molecules still showing some green emission after the exposure to the violet light (spots 1, 7, and 13). For spot 1, quantitative comparison of the intensities shows that the decrease in green matches well with the increase in red fluorescence suggesting that spot 1 consists of a cluster of at least two active fluorophores. Spot 7 shows a brief reactivation of green fluorescence in frame 5 while exhibiting red fluorescence in frames 5–8. This could be explained by transient reactivation from a "dark" state to the intensity comparable with that of frame 1 and a subsequent switching to the red Kaede form. Spot 9 shows conversion already in frame 2, which might have potentially been activated by 488 nm light. Although this seems rather unlikely, it is still possible taking into account the absorption spectrum of other protonated GFP mutants; the protonated molecule is supposed to have the maximum absorption at ~400 nm. Therefore, 405 nm light can efficiently trigger the green-to-red conversion (Ando et al., 2002; Chattoraj et al., 1996; Mizuno et al., 2003). However, the proto-

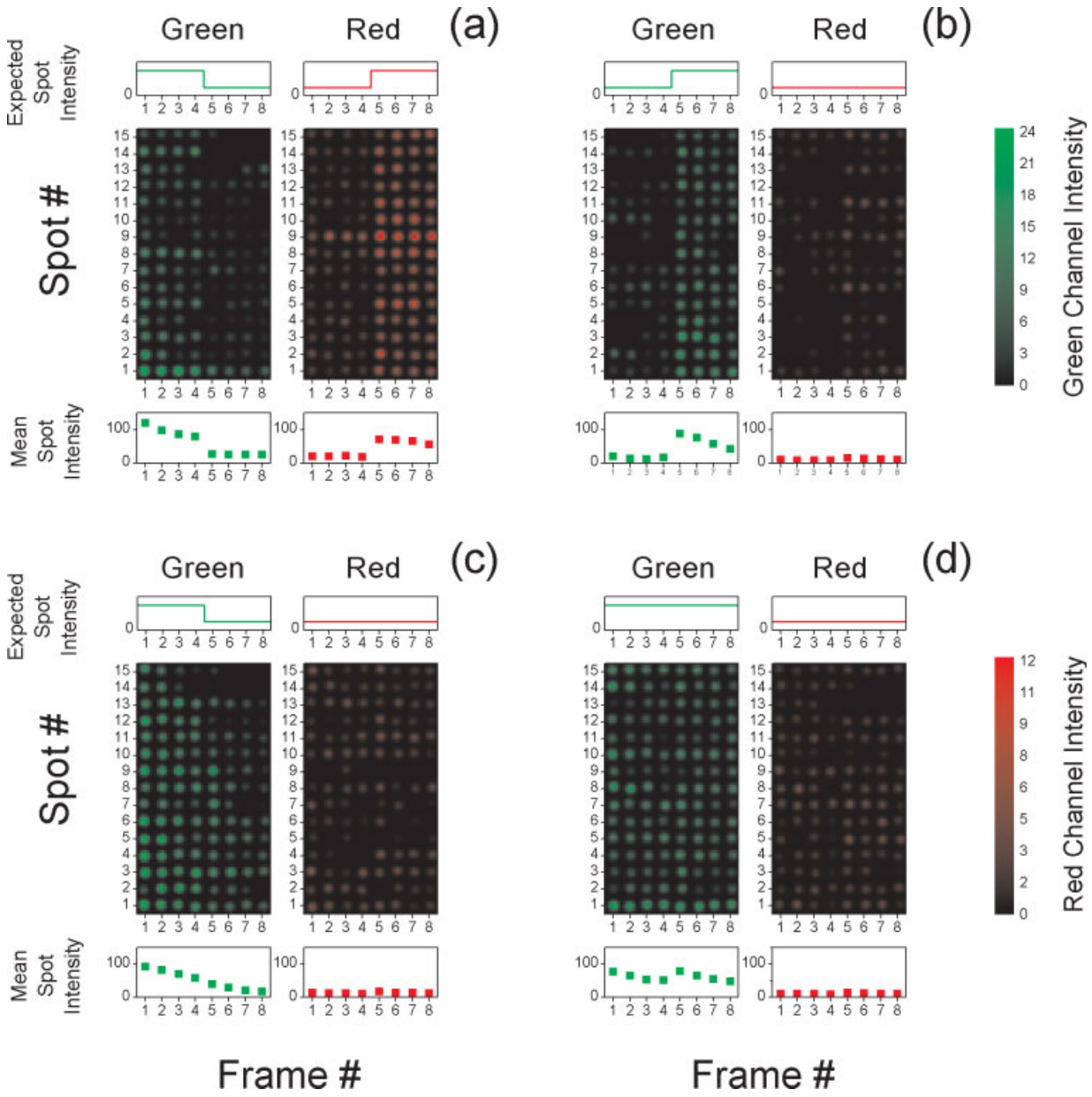


Fig. 6. Reconstructed time sequences of single Kaede molecule images in green and red spectral channels for four most significant groups, classified according to their fluorescence dynamics pattern. Fifteen representative traces are displayed for each group. Schematic representations of the group-specific type of fluorescence dynamics are shown on top of each panel (solid lines). The actual dynamics of the mean spot intensity for each of the groups is shown at the bottom of each panel (squares). In total, 534 intensity traces were analyzed. **a**: Group demonstrating green-to-red photoswitching (22 intensity traces (4%) were detected); **b**: Group exhibiting photoactivation of the green emission with no red emission observed (70 intensity traces (13%) were detected); **c**: Group demonstrating photoinduced deactivation of green emission with no red emission observed (230 intensity traces (43%) were detected); and **d**: Group showing partial photoinduced revival of green emission with no red emission observed (160 intensity traces (30%) were detected). [Color figure can be viewed in the online issue, which is available at www.interscience.wiley.com.]

nated molecule also exhibits (weak) absorption at higher wavelengths, e.g., 488 nm. A slight decrease in the rKaede emission intensity in the red channel in frames 5–8 can be seen in Figure 6a, lower panel, which is indicative of photobleaching of rKaede by 488 nm light.

Besides the green-to-red photoswitching behavior of the Kaede molecules, a substantial amount of the detected Kaede molecules showed activation in the green channel upon illumination by 405 nm light (Fig. 6b). Seventy of 534 traces (13%) were sorted as "green off/on," "red off/off." Intensity in the red channel was dim through the entire eight frames (slight intensity increase in the red channel in frames 5–8 can be attributed to spectral crosstalk from the green channel.) Activation of green fluorescence from a nonfluorescent state seems to be a common feature among GFP mutants as observed before (Jung et al., 2001). In case of the fluo-

rescent protein Dronpa (Habuchi et al., 2005), a high degree of reversibility exists. As traces 2, 6, and 10 shows, re-activation in the green channel occurs after the preceding dimming of the spots in frames 4 and 5. Whether a reversibility (as in case of Dronpa) exists also for Kaede, further investigations will show.

The trajectories displayed in Figure 6c belong to the large group "green on/off," "red off/off." Two hundred and thirty of the 534 trajectories (43%) were sorted into this subset. The spots collected here display a decrease in the green emission after the 405 nm illumination, stronger than on average expected from photobleaching with 488 nm and might be considered as a partial photodeactivation of the green emission. The signal in the red channel remains dim with weak fluctuations around the mean intensity. The partial photodeactivation of green fluorescence observed in this case can be tentatively attributed to irreversible photobleaching of a fraction of Kaede molecules by the violet light pulse. (A specific investigation of the photobleaching of grKaede by 405 nm light was outside the scope of the present study.)

Figure 6d shows the group of spots which the sorting algorithm regarded as "green on/on," "red off/off." The group consisted of 160 traces (30% of the total number of traces). As can be seen, the spots exhibit a continuous emission pattern in the green channel interrupted occasionally by transient blinking in one or two frames. Green fluorescence is not bleached by probe light within the observation time used here. However, the 405-nm light pulse leads to a slight revival of the intensity in the green and/or the red channels. Red channel fluorescence is always dim in this group. Partial revival of green emission observed in Figure 6d poses interesting questions about the nature of these phenomena (red-to-green conversion upon transient increase in green fluorescence?), however, a more detailed investigation is necessary to clarify this behavior.

It should be noted that we observed only very few events which showed emission in the green and red channels simultaneously. We did not include them into our analysis due to the lack of statistical significance.

Under our experimental conditions, we reproducibly obtained a green-to-red conversion ratio which is significantly below the ratio which can be expected according to bulk measurements in aqueous solution performed before by Ando et al. (2002). Additionally, we found an increase in green fluorescence upon illumination with violet light, consistent to observations on GFP and related fluorescent proteins (Dickson et al., 1997; Habuchi et al., 2005; Jung et al., 2001; Patterson and Lippincott-Schwartz, 2002; Schneider et al., 2005) but contrary to what was previously published by Ando et al. (2002).

In particular, in our experiments we applied 405 nm light in a dose of 15 J/cm$^2$ which is comparable to the dose (ten pulses at 1.3 J/cm$^2$) used by Ando et al. (2002). Of 534 spots which we analyzed, 22 (4%) showed a significant increase in the red spectral channel upon illumination with violet light while becoming dim in the green channel. Likewise, 70 (13%) spots significantly increased their emission intensity in the green spectral region without showing red emission.

In comparison, Ando et al. obtained a decrease in bulk fluorescence in the green channel by about 75% and a ~30-fold increase in the red channel (Ando et al., 2002, Fig. 5c), employing similar spectral emission filters. However, while we used 488 nm laser light to excite both the green and the red forms of Kaede, Ando et al. used blue (475 ± 10 nm) and yellow–green (550 ± 15 nm) Xe-lamp light for excitation of grKaede and rKaede, respectively. These differences in the spectral excitation range probably cause an increase in the absolute value of fluorescence in the red channel compared to our experiment. However, this cannot account for the relative changes in red fluorescence intensity (factor 1.5 (here) versus 63 (Ando et al.)). Additionally, the differences in the spectral regions of the excitation and emission channels between the two works also cannot explain why we observe an increase in green emission contrary to the decrease obtained by Ando et al.

One potential reason for the discrepancies in the results observed could be differences in the chemical environment of the single molecules in our experiment as compared to an aqueous solution. As suggested by Habuchi et al. (2005; supplemental material), this could give rise to a changed photophysical behavior. Another explanation could be based on structural or conformational changes of the protein itself potentially induced by the gel mixture or the polymerization reaction. However, since we did not express the protein in-house, it cannot be excluded that the respective changes had already occurred prior to the polymerization reaction.

## CONCLUSIONS

In conclusion, in the present work we introduced a new approach to single-molecule fluorescence microscopy based on massive statistical analysis of intensity trajectories of single molecules, and applied it to study the photoconversion and photobleaching behavior of the fluorescent protein Kaede immobilized in polyacrylamide gel matrix at room temperature.

Statistical analysis of automatically labeled and fitted single molecule intensity trajectories allowed us to characterize the diverse emission dynamics of both Kaede forms, including bleaching, long term blinking, and photoswitching that were not accessible by bulk measurements.

We analyzed photobleaching of single grKaede molecules by determining the number of fluorescent spots and the sum of their intensities as function of time upon illumination at 488 nm. A biexponential fit was required indicating a slightly heterogeneous photodegradation of the grKaede to 488 nm radiation.

Photoswitching behavior was investigated by applying an additional violet light pulse ($\lambda = 405$ nm) to the sample, monitoring simultaneously the fluorescence emission in the green and red channels before and after the violet light pulse.

We found out that under our experimental conditions, only a small fraction of ~4% of all spots detected converted from the green to the red form. One large group (~30%) was neither affected by the blue nor by the violet light pulse. One group showed a photobleaching over time (~43%). Another major group (~13%), however, showed an increase in the emission in the green channel after being illuminated by violet light as observed previously for GFP and related proteins (Dickson et al., 1997; Habuchi et al., 2005; Jung et al., 2001; Patterson et al., 2002; Schneider et al., 2005). Intensity in the red channel changed insignificantly.

However, the green-to-red conversion ratio of single Kaede molecules immobilized in PAA gel presented here deviates significantly from the values obtained in aqueous solution by bulk fluorescence spectroscopy (Ando et al., 2002). Additionally, we observe an increase in green fluorescence upon illumination with violet light, typical for GFP-like fluorescent proteins (Dickson et al., 1997; Habuchi et al., 2005; Jung et al., 2001; Patterson et al., 2002; Schneider et al., 2005), but contrary to observations by Ando et al. (2002).

Although immobilizing fluorophores within PAA- or PVA-gels is widely established to perform single molecule experiments (Dickson et al., 1996; Habuchi et al., 2005; Patterson et al., 2002), a potential reason for the photophysical discrepancies found could be a different chemical environment within the gel matrix as compared to an aqueous solution. Another explanation could be polymerization-induced alteration of the proteins structure or conformation.

## Outlook

For future experiments, expression and purification of the protein should be performed in-house. Maturation processes of the protein have to be monitored more closely to exclude deteriorating effects on fluorescence activity. In particular, the influence of the gel matrix on the photophysical properties of the proteins has to be checked. To get a better insight into the photoconversion process, improvement of time resolution and detector sensitivity is of crucial importance. However, as we could show in the present study, a thorough statistical analysis of the single molecule trajectories is of at least equal importance.

Applying the technique presented here could be easily adapted to study various FPs, which eventually will give new insights in our understanding of the photophysics of fluorescent proteins. Moreover, by application of spectrally resolved fluorescence imaging, tracking of two or more FPs simultaneously could be facilitated in vitro and in vivo, which will allow investigations of intracellular mobility and pathways of proteins with high spatial and temporal resolution.

## ACKNOWLEDGMENTS

We thank Prof. A. Miyawaki and H. Mizuno for kindly providing us the Kaede protein samples. We thank Rainer Heintzmann for fruitful discussions and for adapting his viewer software to our needs.

## APPENDIX

The threshold value to select one part of a trace as "on" or "off" was determined considering grKaede photobleaching behavior upon illumination. In the first series of experiments, we illuminated the sample 30 times by 488 nm at $3 \pm 0.3$ kW/cm$^2$ for 10 ms. To investigate photoconversion, a new sample was exposed eight times for 50 ms to 488 nm light. Illumination intensity was set to $0.6 \pm 0.06$ kW/cm$^2$. Since the dose (illumination intensity $\times$ time) of the blue light was comparable in the experiments analyzing bleaching as well as photoconversion, the effect of grKaede switching to rKaede could be blurred by bleaching. From a monoexponential fit to the data shown in Figure 3, we can roughly estimate a bleaching time of $\tau = 0.12$ s for the illumination intensity applied. Since the dose acquired scales linearly with intensity, the decay time raises by the same factor as the illumination intensity is decreased. Therefore, we assume a five-fold increase of the bleaching time compared to the photobleaching experiments due to the five times lower excitation intensity of 488 nm light when the photoconversion was investigated. With $r = I_{1–4}/I_{5–8} = \exp(T/2\tau)$, where $T = 8 \times 50$ ms $= 0.4$ s is the total illumination time at 488 nm and $\tau = 0.60$ s, we estimate the ratio $r$ between the mean intensity of the first versus the last four frames as $r = 1.4$. Therefore, the threshold value $r = 2$ was set for both channels indicating "switching on" behavior for $I_{1–4}/I_{5–8} < 0.5$ ("switching off" for $I_{1–4}/I_{5–8} > 2$). (Bulk bleaching experiments (data not shown) suggested a similar bleaching rate for rKaede as for grKaede under the conditions applied.)

Based on the threshold criteria, the intensity trajectories were sorted in 16 different groups representing the possible combinations of emission dynamics pattern in each channel.

## REFERENCES

Ando R, Hama H, Yamamoto-Hino M, Mizuno H, Miyawaki A. 2002. An optical marker based on the UV-induced green-to-red photoconversion of a fluorescent protein. Proc Natl Acad Sci USA 99:12651–12656.

Campbell RE, Tour O, Palmer AE, Steinbach PA, Baird GS, Zacharias DA, Tsien RY. 2002. A monomeric red fluorescent protein. Proc Natl Acad Sci USA 99:7877–7882.

Chattoraj M, King BA, Bublitz GU, Boxer SG. 1996. Ultra-fast excited state dynamics in green fluorescent protein: multiple states and proton transfer. Proc Natl Acad Sci USA. 93:8362–8367.

Dickson RM, Norris DJ, Tzeng Y, Moerner WE. 1996. Three-dimensional imaging of single molecules solvated in pores of poly(acrylamide) gels. Science 274:966–968.

Dickson RM, Cubitt AB, Tsien RY, Moerner WE. 1997. On/Off blinking and switching behaviour of single molecules of green fluorescent protein. Nature 388:355–358.

Dittrich PS, Schaefer SP, Schwille P. 2005. Characterization of the photoconversion reaction of the fluorescent protein Kaede on single molecule level. Biophys J 89:3446–3455.

Gross LA, Baird GS, Hoffman RC, Baldridge KK, Tsien RY. 2000. The structure of the chromophore within DsRed, a red fluorescent protein from coral. Proc Natl Acad Sci USA 97:11990–11995.

Habuchi S, Ando R, Dedecker P, Verheijen W, Mizuno H, Miyawaki A, Hofkens J. 2005. Reversible single-molecule photoswitching in the GFP-like fluorescent protein Dronpa. Proc Natl Acad Sci USA 102:9511–9516.

Haupts U, Maiti S, Schwille P, Webb WW. 1998. Dynamics of fluorescent fluctuations in green fluorescent protein observed by fluorescence correlation spectroscopy. Proc Natl Acad Sci USA 95:13573–13578.

Jung G, Mais S, Zumbusch A, Brauchle C. 2000. Two-color fluorescence correlation spectroscopy of one chromophore: application to the E222Q mutant of the green fluorescent protein. J Chem Phys 114:3149–3156.

Kues T, Peters R, Kubitscheck U. 2001. Visualization and tracking of single protein molecules in the cell nucleus. Biophys J 80:2954–2967.

Lossau H, Kummer A, Heinecke R, Pollingerdammer F, Kompa C, Bieser G, Jonsson T, Silva CM, Yang MM, Youvan DC, Michelbeyerle ME. 1996. Time-resolved spectroscopy of wild-type and mutant green fluorescent proteins reveals excited state deprotonation consistent with fluorophore-protein interactions. Chem Phys 213: 1–16.

Malvezzi-Campeggi F, Jahnz M, Heinze KG, Dittrich P, Schwille P. 2001. Light-induced flickering of DsRed provides evidence for distinct and interconvertible fluorescent states. Biophys J 81:1776–1785.

Matz MV, Fradkov AF, Labas YA, Savitsky AP, Zaraisky AG, Markelov ML, Lukyanov SA. 1999. Fluorescent proteins from nonbioluminescent Anthozoa species. Nat Biotechnol 17:969–973.

Mizuno H, Mal TK, Tong KI, Ando R, Furuta T, Ikuro M, Miyawaki A. 2003. Photo-induced peptide cleavage in the green-to-red conversion of a fluorescent protein. Mol Cell 12:1051–1058.

Nienhaus K, Nienhaus GU, Wiedenmann J, Nar H. 2005. Structural basis for photo-induced protein cleavage and green-to-red conversion of fluorescent protein EosFP. Proc Natl Acad Sci USA 102: 9156–9159.

Ormö M, Cubitt AB, Kallio K, Gross LA, Tsien RY, Remington SJ. 1996. Crystal structure of the *Aequorea victoria* green fluorescent protein. Science 273:1392–1395.

Pakhomov AA, Martynova NY, Gurskaya NG, Balashova TA, Martynov VI. 2004. Photoconversion of the chromophore of a fluorescent protein from *Dendronephthya* sp. Biochemistry Mosc 69: 901–908.

Patterson GH, Lippincott-Schwartz J. 2002. A photoactivatable GFP for selective photolabeling of proteins and cells. Science 297:1873–1877.

Schmidt T, Schütz GJ, Baumgartner W, Gruber HJ, Schindler H. 1995. Imaging of single molecule diffusion. Proc Natl Acad Sci USA 93:2926–2929.

Schneider M, Barozzi S, Testa I, Faretta M, Diaspro A. 2005. Tow-photon activation and excitation properties of PA-GFP in the 720–920-nm region. Biophys J 89:1346–1352.

Schwille P, Haupts U, Maiti S, Webb WW. 1999. Molecular dynamics in living cells observed by fluorescence correlation spectroscopy with one- and two-photon excitation. Biophys J 77:2251–2265.

Shagin DA, Barsova EV, Yanushevich YG, Fradkov AF, Lukyanov KA, Labas YA, Semenova TN, Ugalde JA, Meyers A, Nunez JM, Widder EA, Lukyanov SA, Matz MV. 2004. GFP-like proteins as ubiquitous metazoan superfamily: evolution of functional features and structural complexity. Mol Biol Evol 21:841–850.

Shaner NC, Campbell RE, Steinbach PA, Giepmans BNG, Palmer AE, Tsien RY. 2004. Improved monomeric red, orange and yellow fluorescent proteins derived from *Discosoma* sp. red fluorescent protein. Nat Biotechnol 22:1567–1572.

Weiss S. 1999. Fluorescent spectroscopy of single biomolecules. Science 283:1676–1683.

Wiedenmann J, Schenk A, Rocker C, Girod A, Spindler KD, Nienhaus GU. 2002. A far-red fluorescent protein with fast maturation and reduced oligomerization tendency from Entacmaea quadricolor (Anthozoa, Actinaria). Proc Natl Acad Sci USA 99: 11646–11651.

Wiedenmann J, Ivanchenko S, Oswald F, Schmitt F, Rocker C, Salih A, Spindler KD, Nienhaus GU. 2004. EosFP, a fluorescent marker protein with UV-inducible green-to-red fluorescence conversion. Proc Natl Acad Sci USA 101:15905–15910.

Xie XS, Trautman JK. 1998. Optical studies of single molecules at room temperature. Annu Rev Phys Chem 49:441–480.

Zhang J, Campbell RE, Ting AY, Tsien RY. 2002. Creating new fluorescent probes for cell biology. Nat Rev Mol Cell Biol 3:906–918.